Quantum Measurements in Atom Optics*

D. F. Walls

Department of Physics, University of Auckland,
Private Bag 92019, Auckland, New Zealand.

Abstract

We review recent progress in atom optics. We describe new quantum measurements based on the entanglement of quantum states of a light field with atomic external degrees of freedom. Examples include the quantum non-demolition measurement of the photon number in a cavity and the measurement of atomic position.

1. Introduction

In this set of lectures our focus will be on what new kind of quantum measurements are now available to us through the development of atom optics. For a review of atom optics see Adams *et al.* (1994), Wilkens (1995) and Wallis (1995). Much of the theoretical analysis of atom optics requires only a classical treatment of the electromagnetic field. We will investigate new phenomena which arise when the electromagnetic field is quantised (for a general coverage of quantum optics, including quantum measurement and atom optics, see Walls and Milburn 1994). Due to the large de Broglie wavelength of laser-cooled atoms the atomic external degrees of freedom must be treated quantum mechanically. The interaction between the atoms and the light enables entangled states to be formed between both the internal and external degrees of freedom of the atoms and the light field. We shall exploit this entanglement to obtain information on the quantum state of the system by making measurements on the system with which it is entangled.

We shall in the main consider a class of quantum measurements known as quantum non-demolition (QND) measurements (Braginsky 1988; Caves *et al.* 1980) where the act of measurement does not affect the subsequent measurements of the QND variable. We first analyse the QND measurement of the photon number in a cavity by measuring the momentum distribution of atoms deflected by the standing-wave light field. In this case we have an entanglement between the atomic momentum and the quantum states of the light field. A proposal of Brune *et al.* (1990) for a QND measurement of photon number by measuring the atomic (internal) phase relies on the entanglement between the quantum states of the light and the internal degrees of freedom of the atom.

---

* Refereed paper based on a series of lectures presented to the Atom Optics Workshop, held at the Institute for Theoretical Physics, University of Adelaide, in September 1995.

The position of the atom in the standing-wave field may be determined by measuring the phase shift imparted to the light field by the interaction with the atom. In this case we have an entanglement between the atomic position and the phase of the light field. We first consider the situation where the interaction time of the atom with the light field is small so that the transverse motion of the atom in the light field may be neglected (Raman–Nath regime). We then consider longer interaction times where the transverse motion of the atom in the light field is important. In this case a continuous measurement of the phase of the light field tracks the motion of the atom in the standing-wave field.

2. Quantum Non-demolition Measurements

The objective of a quantum non-demolition (QND) measurement is to measure an observable without disturbing it. The back-action noise of the measurement is evaded by shunting it into a complementary observable. The concept of QND measurements was first developed by Braginsky (1988) in the context of the detection of gravitational radiation. He realised that the signal from the gravity wave is so weak as to be obscured by the quantum noise of the measurement. A general theory of QND measurements was developed by Caves *et al.* (1980) who suggested several QND measurement schemes involving coupled mechanical oscillators. However, optical systems have proved the most successful for an experimental realisation of QND measurements. For a review of QND experiments in optics see Grangier (1991). We shall outline the general principles of QND measurements.

The essential requirement of a QND measurement is that it does not affect the precision of subsequent measurements. This leads to the following criterion for a QND observable, that it commutes with itself at a later time,

$$[X(t), X(t')] = 0 \,. \tag{1}$$

Thus for a free particle the momentum p is a QND observable whereas the position is not. For a harmonic oscillator p and x are not QND observables, but the energy E and the quadrature phases X_1 and X_2 are.

A measurement scheme involves coupling an observable X_{s} of a system to a meter or probe. A readout of a probe observable X_{p} gives a measure of the signal observable X_{s}. The coupling should be such that the signal observable is unaffected by the back-action noise of the measurement. This will be the case if the signal observable X_{s} commutes with the signal–probe coupling Hamiltonian,

$$[H_{\mathrm{sp}}, X_{\mathrm{s}}] = 0 \,. \tag{2}$$

In an ideal QND measurement the probe output is detected, giving a measure of the signal input without disturbing the signal output.

3. QND Measurement of Photon Number by Atomic Beam Deflection

We shall consider the deflection of ground-state atoms from the quantum field stored in a standing-wave optical cavity. Meystre *et al.* (1989) have shown that the atomic beam deflection by a light field is a sensitive function of the photon field statistics. Holland *et al.* (1991) have shown that if the frequency of

the light is sufficiently detuned from the atomic resonance and the cavity Q is sufficiently high, the momentum distribution of the scattered atoms constitutes a QND readout of the photon number observable. For the case of a resonant two-level atom, Herkommer *et al.* (1992) have shown that a joint measurement of the atomic momentum and an appropriate field variable allows us to reconstruct the original photon statistics even for this demolition Hamiltonian. Proposals for experiments have been put forward by Treussart *et al.* (1994) and Matsko *et al.* (1994). We shall describe in some detail the proposal of Holland *et al.* (1991). The Hamiltonian for a two-level atom interacting with a quantised cavity field mode is

$$H = \hbar\omega_0\sigma_z + \frac{p^2}{2m} + \hbar\omega a^\dagger a + \hbar\left(g\sigma_- a^\dagger + g^*\sigma_+ a\right)\cos kx\,,\tag{3}$$

where the field mode is described by the boson operator a, the internal degrees of freedom of the atom by the Pauli pseudospin operators σ_+, σ_-, σ_z and g is the dipole coupling constant. We shall assume that the interaction time is sufficiently small that the transverse kinetic energy absorbed by the atom during the interaction can be neglected. This amounts to dropping the $(p^2/2m)$ term. This is known as the Raman–Nath approximation and requires the interaction time $t < 2\pi/\omega_r$, where the recoil energy is $\hbar\omega_r = (2r\hbar k)^2/2m$, where r is an integer.

We shall consider the case of a large detuning $\delta\omega = \omega_0 - \omega$ where spontaneous emission can be neglected and the upper atomic level adiabatically eliminated as follows. Expressing the wavefunction as

$$|\psi\rangle = a\,|e\rangle\,|n-1\rangle + b\,|g\rangle\,|n\rangle\,,\tag{4}$$

where $|e\rangle$ and $|g\rangle$ represent the excited and ground states of the atom, and $|n\rangle$ is a number state of the field. In the Schrödinger picture we have

$$i\hbar\frac{\partial a}{\partial t} = \left[\hbar\omega(n-1) + \tfrac{1}{2}\hbar\omega_0\right]a + \hbar g\sqrt{n}\cos kx\; b\,,\tag{5}$$

$$i\hbar\frac{\partial b}{\partial t} = \left[\hbar\omega n - \tfrac{1}{2}\hbar\omega_0\right]b + \hbar g^*\sqrt{n}\cos kx\; a\,.\tag{6}$$

Transforming to the interaction picture with $\mathcal{H}_0 = \hbar\omega a^\dagger a + \hbar\omega_0\sigma_z$,

$$a_2 = a\,e^{i[(n-1)\omega + \frac{1}{2}\omega_0]t}\,,\tag{7}$$

$$b_2 = b\,e^{i(n\omega - \frac{1}{2}\omega_0)t}\,,\tag{8}$$

these equations become

$$\frac{\partial a_2}{\partial t} = -ig\sqrt{n}\cos kx\; e^{i(\omega_0-\omega)t}\,b_2\,,\tag{9}$$

$$\frac{\partial b_2}{\partial t} = -ig^*\sqrt{n}\cos kx\; e^{-i(\omega_0-\omega)t}\,a_2\,.\tag{10}$$

In order to remove the time dependence in (9) we need the component of $a_2 \sim e^{i(\omega_0-\omega)t}$. This may be derived by the following adiabatic elimination procedure. Integrating (9),

$$a_2(t) = -\int_{-\infty}^{t} ig\cos kx \, e^{i(\omega_0-\omega)\tau} \sqrt{n}\, b_2(\tau)\, \mathrm{d}\tau \,. \tag{11}$$

Integrating by parts,

$$a_2(t) = \left[\frac{-ig\cos kx}{i(\omega_0-\omega)} e^{i(\omega_0-\omega)t} \sqrt{n}\, b_2(t)\right]$$
$$- \int_{-\infty}^{t} \mathrm{d}\tau \sqrt{n} \left(\frac{\partial b_2}{\partial \tau}\right) \left[\frac{-ig\cos kx}{i(\omega_0-\omega)} e^{i(\omega_0-\omega)\tau}\right] \,. \tag{12}$$

Now, $\partial b_2/\partial \tau$ is very small in the large detuning limit and hence we may neglect the second term, thus

$$a_2(t) \approx \frac{-\sqrt{n}\, g\cos kx}{\omega_0-\omega} e^{i(\omega_0-\omega)t} b_2(t) \,. \tag{13}$$

Hence

$$\frac{\partial b_2}{\partial t} = \frac{in\,|g|^2 \cos^2 kx}{\omega_0-\omega} b_2 \,, \tag{14}$$

which is consistent with the effective Hamiltonian

$$H_{\text{eff}} = \hbar\delta\omega\sigma_z + \frac{2\hbar|g|^2}{\delta\omega} \sigma_z a^\dagger a \cos^2 kx \,. \tag{15}$$

We see from this Hamiltonian that the photon number $a^\dagger a$ is a QND observable. It may be determined by measuring either the atomic phase or the outgoing momentum. We shall calculate the outgoing momentum, which is the probe observable in this QND measurement.

The atomic state vector in the coordinate representation may be written as

$$|\psi(t)\rangle = a(x,t)\,|e\rangle + b(x,t)\,|g\rangle \,, \tag{16}$$

where $a(x,t)$ $(b(x,t))$ is the probability amplitude for the atom to be in the excited (ground) state at the transverse coordinate x at time t.

We assume that the atoms are initially in the ground state with a Gaussian wavefunction,

$$a(\xi,0) = 0,$$
$$b(\xi,0) = \left(\pi\sigma^2\right)^{-\frac{1}{4}} \exp\left(-\frac{\xi^2}{2\sigma^2}\right) \,, \tag{17}$$

where $\xi = kx$ and σ is proportional to the rms transverse position spread of the input beam. This may be written as

$$b(\xi, 0) = \left(\frac{2\sigma_\eta^2}{\pi} \right)^{\frac{1}{4}} \exp\left[-(\sigma_\eta \xi)^2 \right], \tag{18}$$

where σ_η is the rms transverse momentum spread of the input beam scaled to the photon number momentum $\hbar k$, $\eta = (p/\hbar k)$. The Schrödinger equation in the large detuning limit is

$$\frac{\partial}{\partial \tau} \begin{pmatrix} a_n \\ b_n \end{pmatrix} = \begin{pmatrix} -i\Delta - i\cos^2\xi/2\Delta & 0 \\ 0 & i\Delta + i\cos^2\xi/2\Delta \end{pmatrix} \begin{pmatrix} a_n \\ b_n \end{pmatrix}, \tag{19}$$

where $\tau = \Omega t$ and $\Delta = (\delta\omega/2\Omega)$. We have assumed that the cavity field initially has n photons so $\Omega = |g|\sqrt{n}$ and the atom interacts with a field of constant amplitude for a time τ. The solution for $b_n(\xi, t)$ is

$$b_n(\xi, t) = \exp\left[i \left(\tfrac{1}{2}\delta\omega + \frac{|g|^2 n}{2\delta\omega} \right) t \right] \sum_{r=-\infty}^{\infty} i^r J_r \left(\frac{|g|^2 n t}{2\delta\omega} \right) \exp\left(2ir\xi \right) b(\xi, 0), \tag{20}$$

or in the momentum representation

$$\tilde{b}_n(\eta, t) = \exp\left[i \left(\tfrac{1}{2}\delta\omega + \frac{|g|^2 n}{2\delta\omega} \right) t \right] \sum_{r=-\infty}^{\infty} i^r J_r \left(\frac{|g|^2 n t}{2\delta\omega} \right) \tilde{b}(\eta - 2r, 0). \tag{21}$$

Since the photon number of the field is unchanged by the interaction, the joint state of the atom and field is

$$\int \tilde{b}_n(\eta, t) |n\rangle |\eta\rangle \, \mathrm{d}\eta. \tag{22}$$

If the initial state is given by a superposition of number states, $\sum c_n |n\rangle$, the final joint state is given by

$$|\psi\rangle = \sum_{n=0}^{\infty} \int c_n \tilde{b}_n(\eta, t) |n\rangle |\eta\rangle \, \mathrm{d}\eta. \tag{23}$$

The probability that the final atomic momentum is $p = \eta\hbar k$ without regard for the field state is given by the following trace:

$$P(\eta) = \mathrm{Tr}(|\psi\rangle\langle\psi| \, |\eta\rangle\langle\eta|) = \sum_{n=0}^{\infty} |c_n|^2 \, |b_n(\eta, t)|^2$$

$$= \sum_{n=0}^{\infty} |c_n|^2 \left| \sum_{r=-\infty}^{\infty} i^r J_r \left(\frac{|g|^2 n t}{2\delta\omega} \right) \tilde{b}(\eta - 2r, 0) \right|^2. \tag{24}$$

If the original momentum uncertainty is so small that $\tilde{b}(\eta, 0)$ is non-zero only when $|\eta| < 1$, then

$$P(\eta) = \sum_{r=-\infty}^{\infty} \left[\sum_{n=0}^{\infty} |c_n|^2 \left| J_r \left(\frac{|g|^2 \, n \, t}{2\delta\omega} \right) \right|^2 \right] \left| \tilde{b}(\eta - 2r, 0) \right|^2 , \qquad (25)$$

which consists of copies of the input beam shifted in momentum by even multiples of $\hbar k$. The amplitudes of these copies are related to the photon number statistics of the light field by $P(n) = |c_n|^2$.

The output momentum distribution $P(\eta)$ is plotted in Fig. 1 for the cavity field in: (a) a number state $N = 10$, (b) a coherent state $\bar{n} = 10$, (c) a thermal state $\bar{n} = 10$. We see that for a number state the momentum distribution consists of a series of peaks corresponding to exchanges of $2r\hbar k$ units of momentum. For a coherent state the distribution is split into two principal peaks. For a thermal state the split of momentum is much smaller.

We see from (24) that the momentum distribution depends on the photon statistics $P(n)$ of the cavity field. This may be exploited to obtain a QND measurement of the photon number by measuring the momentum distribution of the scattered atoms. This is equivalent to the position distribution of the far field. Each atomic position measurement gives some information about the field photon statistics and reduces the density operator of the field. If the cavity lifetime is long compared to the time between atomic injections, (24) can be inverted, and sufficiently repeated measurements will eventually completely determine the photon statistics. If the cavity is not significantly coupled to any external reservoir, continual probing of the cavity by successive atoms will eventually result in the complete collapse of the field state to that of a number state. We shall illustrate this phenomenon by simulating repeated atomic measurements and examining the residual density of states.

For simplicity, we consider a monokinetic atomic beam in which the longitudinal velocity spread is small compared to the mean velocity. The first atom which passes through the cavity acquires an output momentum p_0 which gives us some information on the field statistics. The diagonal elements of the field density matrix $P(n)$ are then altered by the back-projection of the measurement, $P(n|p_0) = M \, P(p_0|n) \, P(n)$, where M is a normalisation constant. The next atom passing through acquires a momentum p_1 and the field density matrix is further reduced. A simulation of a sequence of five atoms and their effect on the field photon distribution is shown in Fig. 2. The number of times that each value of the exit momentum is chosen is completely determined by the initial photon statistics. Note that the measurement of each individual atom's momentum extracts partial information from the field, and it is only the cumulative information contained in the full measurement sequence which contracts the field to a well defined number state.

Requirements for a QND Measurement

The above results are based on the effective Hamiltonian (15) which gives a perfect QND coupling. In order to achieve a near-perfect QND scheme experimentally, the following considerations apply. The atom must be prepared
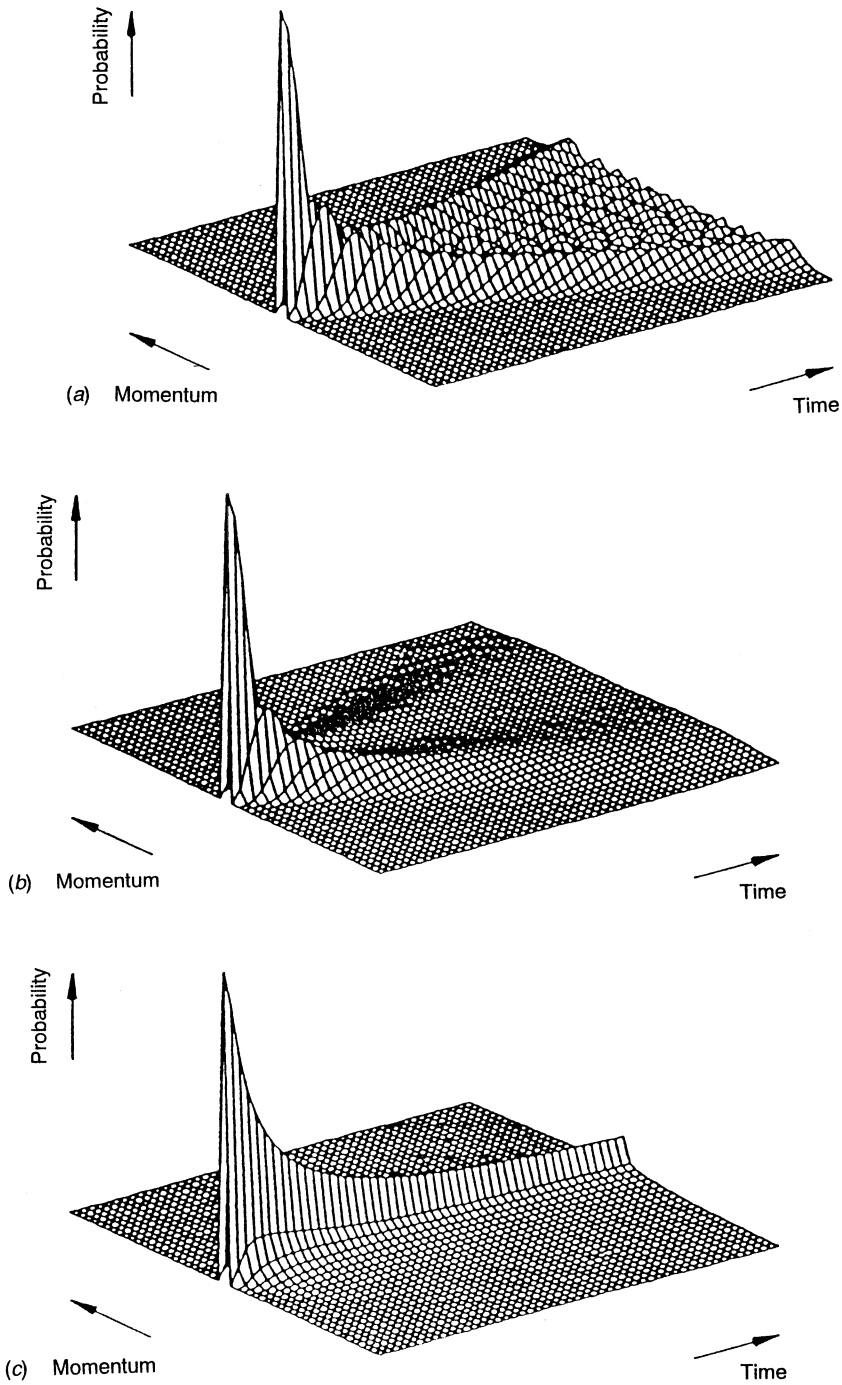
Fig. 1. Output momentum distribution $P(\eta)$ for the cavity field in (a) a number state $N = 10$; (b) a coherent state $\bar{n} = 10$; and (c) a thermal state $\bar{n} = 10$.

in the ground state so that new photons are not deposited into the system. The atomic inversion must be negligible so that the atom does not exit in the excited state carrying off a quantum of energy. This requirement is that $|g|^2 n \ll \delta\omega^2 + \gamma^2$,
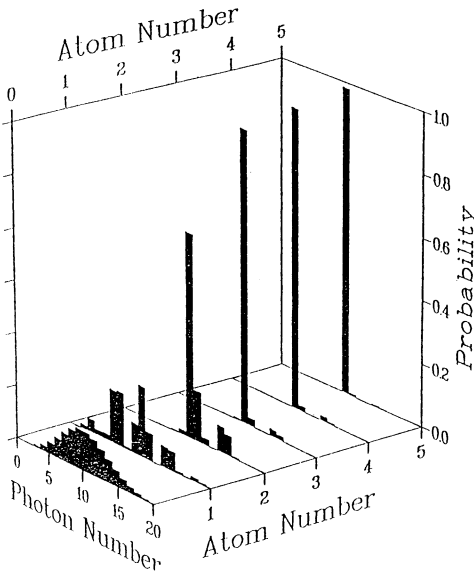
Fig. 2. Photon number distribution $P(n)$ after a measurement of the momentum distribution of a sequence of atoms.

where γ is the spontaneous emission rate, $\delta\omega$ is the detuning and g is the dipole coupling strength. The number of photons spontaneously emitted from the atom while it is in the interaction region must be very small. This requirement is that $|g|^2 n\gamma t/(\delta\omega^2 + \gamma^2) \ll 1$, where t is the interaction time. The atom must be in the field for a sufficient time to allow some interchange of photons, so that there is an appreciable probability of deflection. This requires $|g|^2 nt/2\delta\omega = r$, where r is the characteristic number of $2\hbar k$ units of deflection. Finally, the interaction time must be sufficiently small that the transverse kinetic energy absorbed by the atom during the interaction can be neglected, that is, the Raman–Nath regime must hold. This requires $t < 2\pi/\omega_r$, where the recoil energy is $\hbar\omega_r = (2r\hbar k)^2/2m$, m is the atomic mass, and k is the wave number of the cavity mode.

In addition, the interaction time must be small compared to the cavity lifetime so that there is no appreciable decay of the cavity field during the interaction. This requires a high-Q cavity so that the cavity field is repeatedly probed by a number of atoms in the mean lifetime of a cavity photon. Since we are interested in quantum effects which occur with cavity fields containing only a few photons, we require the dipole coupling g between the light field and the atom to be large for the whole effect to be observable. Since the dipole force per photon is inversely proportional to the volume occupied by the field, this leads to the requirement of very small cavities. A promising proposal is to construct cavities using silica microspheres with very-high-Q whispering-gallery modes.

Quality factors $Q \approx 2 \times 10^9$ have been achieved in quartz microspheres. In these whispering-gallery modes (WGMs) light circulates in a thin annular region near the equator, just inside the surface of the sphere. WGMs have a small evanescent component that propagates just outside the surface of the sphere. The high Qs and extremely small electromagnetic mode volumes obtainable in quartz microspheres make them prime candidates for experiments in QND detection.

The parameters for the scheme proposed by Treussart *et al.* (1994) using rubidium atoms are as follows. The radius of the sphere $R = 17 \cdot 5\ \mu$m. The

WG mode has a wavelength $\lambda = 0\cdot78\ \mu$m, near-resonant with the $5S_{\frac{1}{2}} \to 5P_{\frac{3}{2}}$ transition of rubidium. The field at a distance $r > R$ from the sphere's centre decreases exponentially as $\exp[-(r-R)/L]$ with $L = 0\cdot12\ \mu$m. The effective mode volume $V = 160\ \mu$m^3. The field per photon at the surface is $E = 24\ \mathrm{V\,cm}^{-1}$. The equivalent dipole matrix element for a light field detuned by several hundred megahertz from the atomic transition is 2 a.u. This gives a maximum Rabi frequency for a one-photon field

$$\Omega_{\mathrm{max}} = \frac{DE}{\hbar} = 4\cdot4 \times 10^8\ \mathrm{s}^{-1}\,.$$

This becomes $\Omega_{\mathrm{max}}\sqrt{n}$ when n photons are present.

A similar scheme proposed by Mabuchi and Kimble (Mabuchi and Kimble 1994; Kimble 1994) leads to the following parameters for caesium atoms. For a sphere of radius $R = 9\ \mu$m they estimate that a $g/\gamma = 50$ would be possible. If a Q factor of 10^{11} is achievable this would give $g/\kappa \approx 7 \times 10^4$, where κ is the cavity decay rate. For comparison the highest reported values (Kimble 1994) achieved with caesium atoms in a Fabry–Perot cavity are $g/\gamma = 2\cdot9$, $g/\kappa = 12$.

4. Localisation of Atomic Position

We now consider a method to localise the position of an atom using the interaction with a light field. If the position of the atom is determined by observing light scattered from an atom (the Heisenberg microscope), the position cannot be localised to better than a wavelength. Alternative methods to make atomic position measurements using an optical field include channelling in an off-resonant optical standing wave (Salomon *et al.* 1987) and spatially varying level shifts, which enable one to correlate the atomic position with its resonance frequency (Gardner *et al.* 1993). In this paper we shall describe a quantum measurement of the atom's position to better than a wavelength resolution by measuring the phase of the light field (Storey *et al.* 1992, 1993; Marte and Zoller 1992).

When a two-level atom is passed through a standing-wave mode in an optical cavity the interaction with the field depends on the position of the atom. By measuring the quadrature phase X_1 of the field it is possible to localise the position of the atom very precisely within a wavelength of the light in the cavity.

We consider the large detuning limit and work in the Raman–Nath regime where the effective Hamiltonian is given by (15). The cavity mode is assumed to be initially in a coherent state $|\alpha\rangle$. The atom is assumed to be initially in the ground state with a transverse spread in position given by $\phi(x)$. Using the following notation for the field state and the position and internal states of the atom,

$$|\text{field, position, internal}\rangle \equiv |\text{field}\rangle \otimes |\text{position}\rangle \otimes |\text{internal}\rangle\,,$$

we can write the initial state of the system as

$$|\psi(0)\rangle = \int \mathrm{d}x\,\phi(x)\,|\alpha,\ x,\ 0\rangle\,.$$

After an interaction time t in the field, the state of the system is

$$|\psi(t)\rangle = \int dx\, \phi(x) \exp\left[-\frac{iV_i t}{\hbar}\right] |\alpha,\, x,\, 0\rangle$$

$$= \int dx\, \phi(x)\left|\alpha \exp\left[i\frac{|g|^2 t}{\Delta}\cos^2(kx)\right],\, x,\, 0\right\rangle. \qquad (26)$$

Because the interaction with the field is dependent on the position of the atom, a measurement of the quadrature phase $X_1 = a + a^\dagger$ of the field localises the atom. To find the atomic state after the field measurement, we project the field state onto an eigenstate $|X_1\rangle$ of the quadrature phase:

$$|\psi(t)\rangle_{\text{atom}} = \left\langle X_1 \left| \alpha \exp\left[i\frac{|g|^2 t}{\Delta}\cos^2(kx)\right]\right.\right\rangle |x,\, 0\rangle$$

$$= \int dx\, \phi(x)\frac{1}{\sqrt[4]{2\pi}}\exp\left\{-\left[\left(\alpha_1 - \frac{X_1}{2}\right)^2 + i\alpha_2\left(\alpha_1 - X_1\right)\right]\right\} |x,\, 0\rangle, \qquad (27)$$

where

$$\alpha_1 + i\alpha_2 = \int dx\, \phi(x)\, \alpha \exp\left[i\frac{|g|^2 t}{\Delta}\cos^2(kx)\right]. \qquad (28)$$

In order to observe the correlation between the atomic position and the value of the quadrature phase, the transit time of each atom through the cavity must be much shorter than the lifetime of the cavity, which in turn must be much shorter than the interval between the times that successive atoms enter the cavity, i.e.

$$t \ll \tau_{\text{cavity}} \ll \Delta T, \qquad (29)$$

where ΔT is the time interval between successive atom injections.

We assumed that the transverse motion of the atom is negligible during the interaction. This requirement can be expressed as

$$\Delta x \ll \lambda, \qquad (30)$$

where Δx is the uncertainty in the transverse distance travelled by the atom during the interaction time.

If the scheme is implemented at optical wavelengths, this Raman–Nath condition imposes a severe restriction on the interaction time and the field strength. Therefore, to observe any atomic localisation we require the atom–field coupling constant to be extremely high. To calculate how high the coupling constant needs to be, we must estimate the uncertainty introduced into the atom's transverse position during the interaction.

We will assume that

$$\frac{|g|^2 t}{\Delta} = \pi \tag{31}$$

because this condition gives the best localisation.

The transverse-momentum probability distribution of the atom after the interaction in the cavity can be calculated numerically, and the momentum uncertainty is found to be approximately proportional to the field strength. We can then write $\Delta p \approx \eta \langle n \rangle \hbar k$, where Δp is the transverse momentum uncertainty of the atom after crossing the cavity, $\langle n \rangle$ is the mean number of photons in the field and η is a proportionality factor to be determined numerically. The transverse-position uncertainty of the atom after the interaction is $\Delta x \approx \Delta p\, t / 2m$ and the Raman–Nath condition (30) can be written, after some manipulation, as

$$t \ll \frac{\lambda^2 m}{\pi \hbar \eta \langle n \rangle} \, . \tag{32}$$

The other requirement is that the population of the excited state be negligible. This is satisfied provided the following condition holds:

$$\frac{4 \langle n \rangle |g|^2}{\Delta^2} \ll 1 \, . \tag{33}$$

Substituting for Δ in (33) using (31) gives

$$\frac{4 \pi^2 \langle n \rangle}{|g|^2 t^2} \ll 1 \, . \tag{34}$$

If we now substitute t from the Raman–Nath condition (32), we obtain

$$|g| \gg 2 \langle n \rangle^{\frac{3}{2}} \frac{\pi^2 \eta \hbar}{\lambda^2 m} \, . \tag{35}$$

Assuming (31) we can obtain significant localisation if the mean number of photons in the field is greater than about 8.

For optical transitions the required value for $|g|$ is extremely high (of the order of 10^8 Hz). Such high values have recently been obtained by Yuen (1983) using a very short cavity of high finesse.

Fig. 3 shows the atomic position probability distribution resulting from two different possible measurements of the quadrature phase X_1: (a) $X_1 = -2\alpha$, (b) $X_1 = 0$. The distributions are calculated using the parameters $|\alpha|^2 = 8$, $(g^2 t / \Delta) = \pi$. Better resolution is obtained for a field measurement $X = 0$ than for field measurements $X = \pm \alpha$. The field measurement $X = 2\alpha$ localises the atom at a node of the standing wave, and the measurement $X = -2\alpha$ localises the atom at an antinode of the standing wave. At both the nodes and antinodes of the standing wave, the field intensity changes slowly with position and poor resolution is obtained. For the field measurement $X = 0$ the atom is localised
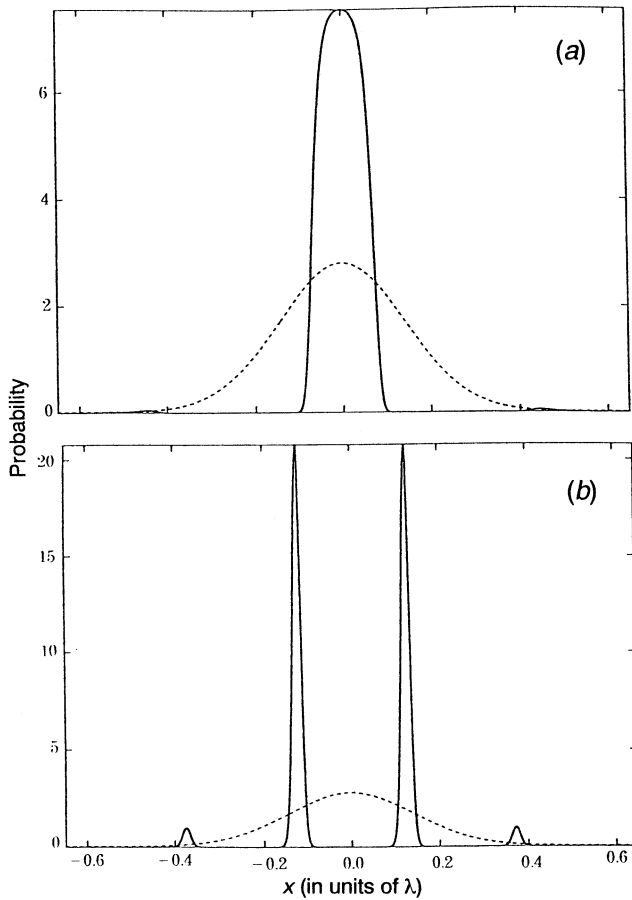
Fig. 3. Position probability distribution of atoms after measurement of the quadrature phase of the light: (a) $X_1 = -2\alpha$ ($\alpha = \sqrt{8}$); (b) $X_1 = 0$. The dotted curves show the initial position distributions.

midway between a node and an antinode of the standing wave, where the field intensity changes rapidly with position and good resolution is obtained.

The initial position distribution $\phi(x)$ was taken to be Gaussian with standard deviation $\sigma = 0 \cdot 9\lambda/2\pi$. This requires that the atoms be cooled before entering the cavity. It is evident that a quadrature phase measurement can localise the atom to a small fraction of a wavelength of the cavity mode. The higher the atom–field coupling constant, the higher we can make the intensity of the field without violation of the Raman–Nath condition, and the better the localisation.

If the atom is allowed to propagate through free space for a time t' after passing through the cavity, then the final state of the atom is

$$\rho_{\text{atom}}(t') = U(t')\, \rho_{\text{atom}}(0)\, U^\dagger(t')\,, \tag{36}$$

where

$$U(t') = \exp\left(-\frac{it'}{\hbar}\frac{p^2}{2m}\right) \tag{37}$$

and $\rho_{\text{atom}}(0)$ is the density operator of the atom alone immediately after it leaves the cavity.

If a measurement on the field is made and a value X_1 is obtained, then $\rho_{\text{atom}}(0) = |\psi(t)\rangle_{\text{atom}} \langle\psi(t)|_{\text{atom}}$, where $|\psi(t)\rangle_{\text{atom}}$ is given in (27). If no field measurement is made, then $\rho_{\text{atom}}(0)$ can be found by tracing over the field states:

$$\rho_{\text{atom}} = \text{Tr}_{\text{field}}\left\{|\psi(t)\rangle\,\langle\psi(t)|\right\} = \exp\left(-|\alpha|^2\right) \int\int \mathrm{d}x\,\mathrm{d}x'\,\phi^*(x')\,\phi(x)\,|x,\ 0\rangle\,\langle x',\ 0|$$

$$\times \exp\left\{|\alpha|^2 \exp\left[i\frac{|g|^2}{\Delta}\,t\,\left(\cos^2 kx - \cos^2 kx'\right)\right]\right\}.\tag{38}$$

Fig. 4a shows the far-field position probability distribution of the atom if no field measurement is made. The far-field position distribution corresponds to the atomic momentum distribution. Figs 4b and 4c show the far-field position probability distribution of the atom for two different possible field measurements. The distinctive shapes of the distributions are due to the rapid oscillations in phase across the atomic wave front as the atom leaves the cavity.

We have shown that a quadrature phase measurement on the field can localise the position of the atom in the near field very precisely within a wavelength of the cavity field. However, a single field measurement cannot determine 'which wave' the atom went through. For example, a field measurement might determine with great precision that the atom went through a node of the cavity mode, but it cannot specify which node. Our position localisation scheme is in this sense a complement of the ideal Heisenberg microscope.

Rydberg atoms also satisfy the requirements for the position measurement scheme. Because Rydberg atoms have huge electric-dipole matrix elements, coupling constants as high as 500 kHz can be achieved. Rydberg atoms also have very long spontaneous emission times (of the order of 10^{-2} s for circular atoms), so long atom–field interaction periods can be achieved. The resonant frequencies between the Rydberg levels fall in the millimetre domain, and suitable cavities can be constructed with lifetimes even longer than the atomic lifetime. Because of the long wavelength of the Rydberg transitions, the Raman–Nath condition is easily satisfied. However, because the wavelengths are much larger than a reasonable atomic de Broglie wavelength, we cannot expect any phase coherence over the initial atomic distribution, which is assumed to be spread over a distance of the order of a wavelength of the cavity mode. In this case the scheme described above behaves as a classical position measurement of the atom rather than a quantum localisation, and there is no interference in the far field.

We have shown that by passing a two-level atom through a standing-wave mode in a cavity and measuring the quadrature phase of the field, we can localise the position of the atom to a fraction of a wavelength of the light in the cavity. The most significant factor limiting the degree of localisation achievable in the optical regime appears to be the requirement of a very high atom–field coupling constant.
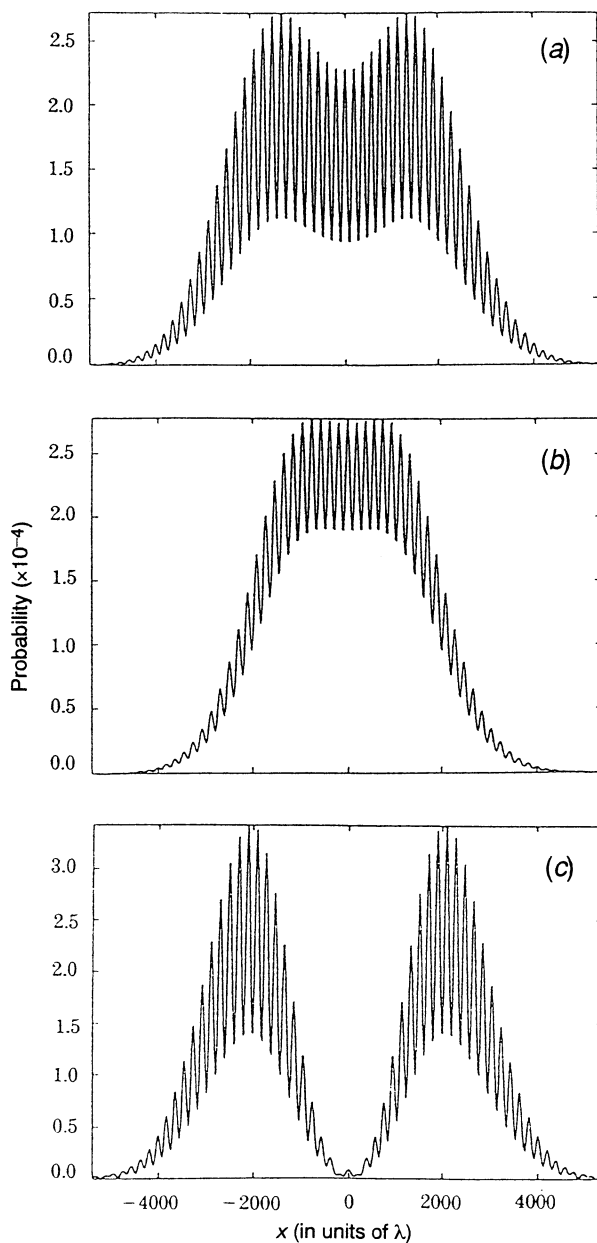
Fig. 4.   (a) Far-field position probability distribution of the atom
if no field measurement is made; (b) far-field position probability
distribution of the atom for quadrature field measurement, with
$X_1 = -2\alpha$; and (c) as for (b), but with $X_1 = 0$.

5. Contractive States

The standard quantum limit, as it was originally formulated by Caves *et al.*
(1980), states that in two successive position measurements of a free mass m

made a time τ apart, the result of the second measurement cannot be predicted with uncertainty smaller than $(\hbar\tau/m)^{\frac{1}{2}}$. A heuristic argument for this limit runs as follows. The uncertainty in the position of a mass at a large time τ after a position measurement will arise from two sources: there will be some uncertainty due to the finite resolution $\Delta x(0)$ of the first measurement, and there will be a contribution $\Delta p(0)\tau/m$ from the momentum uncertainty introduced by the measurement. The resulting uncertainty obtained by combining these two contributions is

$$\Delta x(\tau) = \sqrt{\Delta x^2(0) + \Delta p^2(0)\left(\frac{\tau}{m}\right)^2}.\tag{39}$$

$\Delta x(\tau)$ can be minimised by varying the initial position and momentum uncertainties within the constraint imposed by the uncertainty principle. According to this argument, the position uncertainty at time τ must therefore be greater than a minimum given by

$$\left\langle\Delta x^2(\tau)\right\rangle_{\text{SQL}} = \frac{\hbar\tau}{m}.\tag{40}$$

Yuen (1983) pointed out a serious flaw in this heuristic argument for the standard quantum limit. A rigorous treatment of the evolution of a free mass in the Heisenberg picture shows that the position varies as

$$x(t) = x(0) + p(0)\frac{t}{m},\tag{41}$$

where x and p are now quantum mechanical operators. The position uncertainty at time t is therefore

$$\left\langle\Delta x^2(\tau)\right\rangle = \left\langle\Delta x^2(0)\right\rangle + \left\langle\Delta p^2(0)\right\rangle\frac{t^2}{m^2}$$

$$+ \left\langle\Delta x(0)\Delta p(0) + \Delta p(0)\Delta x(0)\right\rangle\frac{t}{m}.\tag{42}$$

This full treatment reveals a third contribution to the position uncertainty that depends on the correlation between the position and momentum. This correlation was implicitly assumed to be non-negative in the heuristic treatment of the SQL. Indeed it is identically zero if the measurement leaves the mass in a minimum-uncertainty state (which, for the purposes of this paper, we have taken to mean a state satisfying $\Delta x^2\Delta p^2 = \hbar^2/4$).

Yuen described a class of states which can breach the SQL. These states, which he called 'contractive states', have a negative position–momentum correlation that causes them to contract with time. This contraction does not occur indefinitely, but stops when a certain minimum position variance is reached, after which time the state spreads out in the usual manner.

Yuen defined one set of such states, which he termed 'twisted coherent states', in analogy with the squeezed states of the electromagnetic field. These twisted

coherent states may alternatively be thought of as minimum-uncertainty states of a free mass that have been propagated backwards in time.

Suppose that at time $t = 0$ a free mass is in a minimum-uncertainty state with position uncertainty σ. Then at an arbitrary time t the correlation between the position and momentum of the mass is given by

$$\langle \Delta x \Delta p + \Delta p \Delta x \rangle = \frac{\hbar^2 t}{2m\sigma^2} \,, \tag{43}$$

which for $t < 0$ is negative, as required for a contractive state. In fact the states of the mass for $t < 0$ form the set of twisted coherent states. Their position uncertainty decreases while t is negative, reaching a minimum at $t = 0$. This minimum position uncertainty is analogous to a beam waist in optics, and we denote it by w. For positive t the distribution spreads out again.

Producing Contractive States with a Quadratic Potential

We have shown in Section 3 that the position of an atom may be measured by passing it through a standing light wave that is highly detuned from the atomic resonance. In the large detuning and Raman–Nath regime the effective Hamiltonian is given by (15). The state of the system after the interaction is given by

$$|\Psi\rangle = \int \mathrm{d}x \, \kappa(x) e^{-(iHt/\hbar)} |\alpha\rangle \otimes |x\rangle$$

$$= e^{(i\Delta t/\hbar)} \int \mathrm{d}x \, \kappa(x) \left| \alpha e^{i(|g|^2 t/\Delta) \cos^2(kx+\xi)} \right\rangle \otimes |x\rangle \,. \tag{44}$$

The interaction establishes a correlation between the position of the atom and the phase of the field. Information about the atomic position may then be obtained by measuring the quadrature phase $X_\theta = a e^{-i\theta} + a^\dagger e^{i\theta}$ using balanced homodyne detection. Denoting the result of the field quadrature measurement by χ_θ, we can calculate the state of the atom after the field measurement by projecting the system onto the quadrature phase eigenstate $|\chi_\theta\rangle$:

$$|\psi\rangle_{\mathrm{atom}} = N \langle \chi_\theta | \Psi \rangle = N \int \mathrm{d}x \, \kappa(x) \left\langle \chi_\theta \left| \alpha e^{i(|g|^2 t/\Delta) \cos^2(kx+\xi)} \right\rangle \right| x\rangle$$

$$= N \int \mathrm{d}x \, \kappa(x) \frac{1}{\sqrt[4]{2\pi}} \exp \left\{ - \left[\left(\alpha_1 - \frac{\chi_\theta}{2} \right)^2 + i\alpha_2 \left(\alpha_1 - \chi_\theta \right) \right] \right\} |x\rangle \,, \tag{45}$$

where

$$\alpha_1 + i\alpha_2 \equiv \alpha \exp \left\{ i \left[\frac{|g|^2 t}{\Delta} \cos^2(kx + \xi) - \theta \right] \right\} \tag{46}$$

and N is a normalisation factor.

Provided the atomic beam is not too rapidly diverging as it enters the cavity, a field measurement that localises the atom in the region of a field antinode will
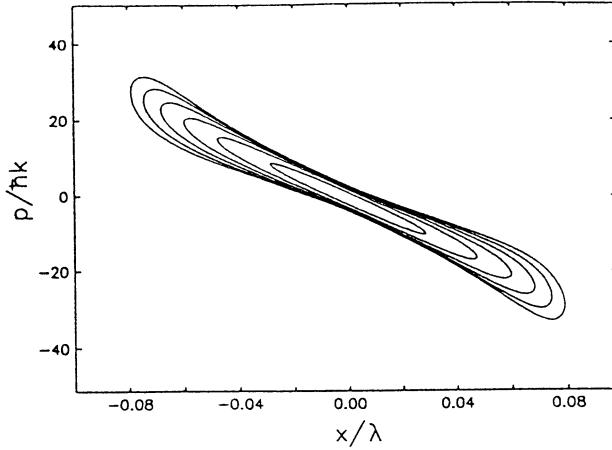
Fig. 5. Atomic Wigner distribution after the field quadrature measurement, with $X_0 = -2\alpha$ ($\alpha = \sqrt{8}$, $|g|^2 t/\Delta = \pi$). The initial atomic state was chosen to be a minimum uncertainty state centred at an antinode with position uncertainty $\sigma = \lambda/4\pi$. The contour levels are spaced logarithmically.
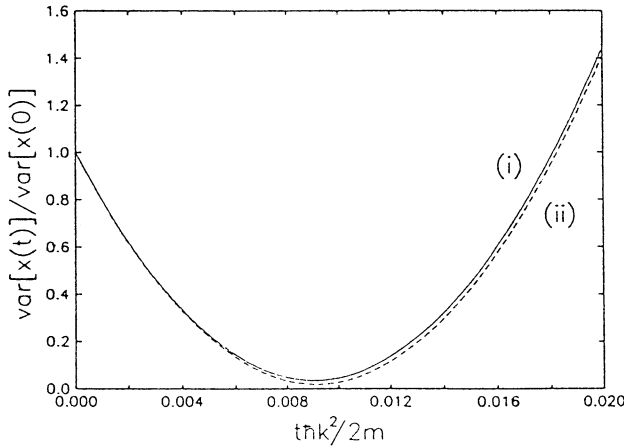

Fig. 6. (i) Evolution of the atomic position variance after the field quadrature measurement. (ii) Focusing of a twisted coherent state.

simultaneously project it into a contractive state. If a higher-intensity field is chosen the atom will be better localised. The potential sampled by the atom will then be more nearly quadratic, and the contractive state into which the atom is projected will more closely approximate Yuen's ideal twisted coherent state.

Fig. 5 shows the Wigner distribution of the atom after a measurement of the field quadrature has localised it at an antinode. The Wigner distribution clearly shows the negative correlation between the position and momentum of the atom. Fig. 6 shows the variance of the atomic distribution as it propagates freely after leaving the cavity. The distribution contracts until it reaches a 'waist', beyond

which it spreads. This is compared with the ideal focusing achieved by a twisted coherent state with the same momentum variance (dashed curve).

We may obtain an estimate of the focal length as follows. We take the field to be initially in a coherent state $|\alpha\rangle$. The process of atom–field interaction and field measurement multiplies the atomic wavefunction by the vector

$$\left\langle X_\theta \middle| \alpha \exp\left(i\frac{|g|^2 t}{\Delta}\cos^2 kx\right)\right\rangle = \sqrt[4]{2\pi}\exp\left[-\left(\alpha_1 - \frac{X_\theta}{2}\right)^2 - \alpha_2\left(\alpha_1 - X_\theta\right)\right], \tag{47}$$

where $\alpha_1 + i\alpha_2 \equiv \alpha \exp i\left([|g|^2 t/\Delta]\cos^2 kx - \theta\right)$ and we have set $\xi = 0$.

Suppose that $\theta = 0$ with α real. Then a field measurement of $X_0 = -2\alpha$ will localise the atom about the point $x = 0$ which is an antinode of the field. The equivalent focal length is determined by the change in phase $\phi(x)$ across the atomic distribution. The phase introduced by the localisation scheme is

$$\phi(x) = -\alpha_2\left(\alpha_1 - X_\theta\right) = -\alpha_2\left(\alpha_1 + 2\alpha\right). \tag{48}$$

Expanding $\phi(x)$ about the antinode of the field $(x = 0)$ to first order,

$$\cos^2 kx \approx 1 - \frac{(kx)^2}{2}. \tag{49}$$

Setting $(|g|^2 t/\Delta) = \pi$ we find, to lowest order,

$$\alpha_1 + 2\alpha = \alpha\cos\left(\cos^2 kx\right) + 2\alpha \approx \alpha, \tag{50}$$

$$\alpha_2 = \alpha\sin\left(\cos^2 kx\right) \approx \pi\alpha\frac{(kx)^2}{2}, \tag{51}$$

which gives the phase across the atomic wavefront to lowest order as

$$\phi(x) \approx -\pi\alpha^2\frac{(kx)^2}{2}. \tag{52}$$

The parabolic dependence of the phase on x indicates focusing. The negative sign shows that an antinode of the standing wave behaves as a converging atomic lens. The effective focal length is

$$f \sim -kx\left(\frac{d\phi}{dx}\right)^{-1} \sim \frac{1}{4\pi\alpha^2 k}. \tag{53}$$

We see that the focal length is inversely proportional to the intensity of the field.

The focusing of the atom described above is largely independent of the field measurement, and essentially results from the quadratic nature of the effective potential at the field antinode. The focusing of atomic beams by standing waves has been observed by Sleator *et al.* (1992). The standing wave used for their

experiment was created by reflecting a travelling wave off a mirror at grazing incidence. The periodicity of the resulting intensity grating was $\approx45\,\mu$m, much larger than the wavelength of the light used. A lens aperture ($25\,\mu$m) was centred in one antinode of the standing wave, and irradiated through a $2\,\mu$m-wide object structure. The atomic beam was focused down to a spot size of $4\,\mu$m.

Measurement-induced Contractive States with a Linear Potential

In this subsection we show that position measurements made using a linear potential can also project a particle into a contractive state (Storey *et al.* 1994). We analyse the same scheme as was discussed in the preceding subsection, but now consider measurements that localise the atom in the region midway between a node and an antinode of the standing wave, where the potential varies linearly with position. In this case focusing may be exhibited by all the conditional atomic distributions (conditioned on the result of the field measurement), but not by the total distribution (obtained when no field measurement is made). We therefore describe the atomic focusing as being measurement-induced. The degree of focusing depends on which field quadrature is measured, that is, it depends on the phase chosen at the homodyne detector.

We suppose that the atom passes through the standing light wave in the region midway between a node and an antinode. If the initial atomic distribution $\kappa(x)$ is sufficiently narrow we need consider only the linear component of the potential. We therefore approximate the field mode by the linear function

$$\cos^2\left(kx - \pi/4\right) \approx kx + \tfrac{1}{2}\,. \tag{54}$$

In our calculation of the atomic state after the interaction and field measurement, we will assume that $|g|^2 t/\Delta = \pi$. Substituting approximation (54) into (46) then gives

$$\alpha_1 = -\alpha\sin\left(\pi kx - \theta\right),$$

$$\alpha_2 = \alpha\cos\left(\pi kx - \theta\right). \tag{55}$$

The state into which the atom is projected by the field measurement is calculated by inserting these expressions for α_1 and α_2 into (45). In keeping with our assumption that the initial atomic distribution $\kappa(x)$ is very narrow, we neglect terms of higher than second order in x in the exponent. For large α we find that the atomic state after the field measurement is given by

$$|\psi\rangle_{\mathrm{atom}} = N \int \mathrm{d}x\, \kappa(x)\, \exp\left\{-\frac{\left[\alpha(\pi kx - \tan\theta) + \chi_\theta/2\cos\theta\right]^2}{1 + i\tan\theta}\right\}$$

$$\times \exp\left\{i\alpha\left[\alpha(\pi kx - \tan\theta) + \frac{\chi_\theta}{\cos\theta}\right]\right\}|x\rangle\,. \tag{56}$$

If the initial distribution $\kappa(x)$ is Gaussian then the state into which the atom is projected by the field measurement is precisely a twisted coherent state.

Calculating the resolution of the position measurement from (56) gives

$$\delta x = \frac{1}{|2\alpha\pi k\cos\theta|}.\tag{57}$$

The best resolution is obtained for an amplitude quadrature measurement (corresponding to $\theta = 0$). The resolution worsens as θ is increased, until in the limit of a phase quadrature measurement ($\theta = \pi/2$) no position information is obtained from the field measurement. Hence in the parameter regime considered in this section we cannot rightly describe a perfect phase quadrature measurement as a position measurement of the atom.

We will take the initial atomic wavefunction $\kappa(x)$ to be that of a minimum-uncertainty state, with momentum uncertainty σ_p,

$$\kappa(x) = \sqrt[4]{\frac{2\sigma_p^2}{\pi\hbar^2}}\exp\left[-\left(\frac{x\sigma_p}{\hbar}\right)^2\right].\tag{58}$$

If θ is chosen so that $\tan\theta$ is negative, then $|\psi\rangle_{\mathrm{atom}}$ in (56) is a contractive state. Since it has a Gaussian position distribution, the effective focal length can easily be calculated. The focal length (in terms of the longitudinal momentum p) is given by

$$f = \frac{-\tan\theta}{2(\alpha\pi k)^2}\frac{p}{\hbar},\tag{59}$$

where it must be remembered that we have set $|g|^2 t/\Delta = \pi$.

Fig. 7 shows the evolution of the atomic position distribution for a field quadrature measurement $X_\theta = 2\alpha\sin\theta$ (the most probable result). Note that the mean momentum differs between the two cases. If the atomic distribution is not conditioned on the result of the field measurement then no focusing is observed, as expected from a linear potential.

Welcher Weg Information

The position localisation scheme presented in this subsection can be used to determine which slit of a double-slit arrangement an atom has passed through. If one slit is located immediately ahead of a node of the standing-wave field and the other slit is located immediately ahead of an antinode, as shown in Fig. 8, then *Welcher Weg* information (which-path information) is recorded in the phase of the field. It is found that as the position of the atom is determined with greater certainty, the visibility of the interference fringes decreases, in accordance with Bohr's principle of complementarity (Bohr 1935).

In the absence of the cavity, the usual double-slit interference pattern is observed in the far field (see Fig. 9). Suppose now that the optical cavity is inserted behind the double slit. The cavity is initially in a coherent state $|\alpha\rangle$, with α real. If the atom passes through the slit located at a node of the standing wave, no interaction occurs and the phase of the field is unaffected. However, if the atom passes through the slit located at an antinode of the standing wave,
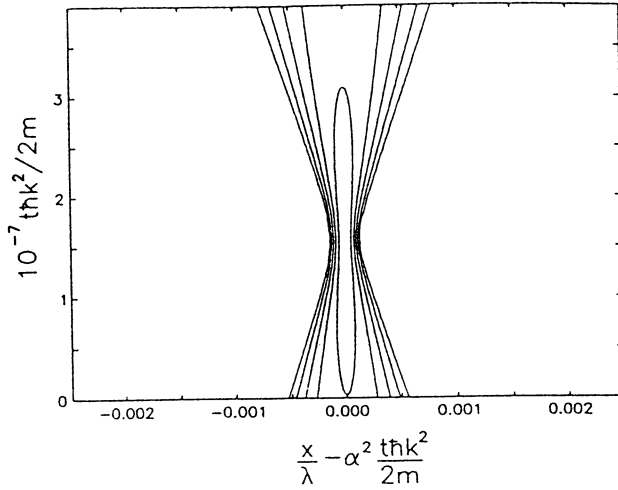
Fig. 7. Evolution of the atomic position distribution after the field quadrature measurement $X_\theta = 2\alpha \sin\theta$, for $\theta = 0\cdot45\pi$, $\alpha = 10^3$ and $|g|^2 t/\Delta = \pi$. The initial atomic state was chosen to be a minimum-uncertainty state centred midway between a node and antinode with momentum uncertainty $\sigma_p = \alpha\pi\hbar k/10$.
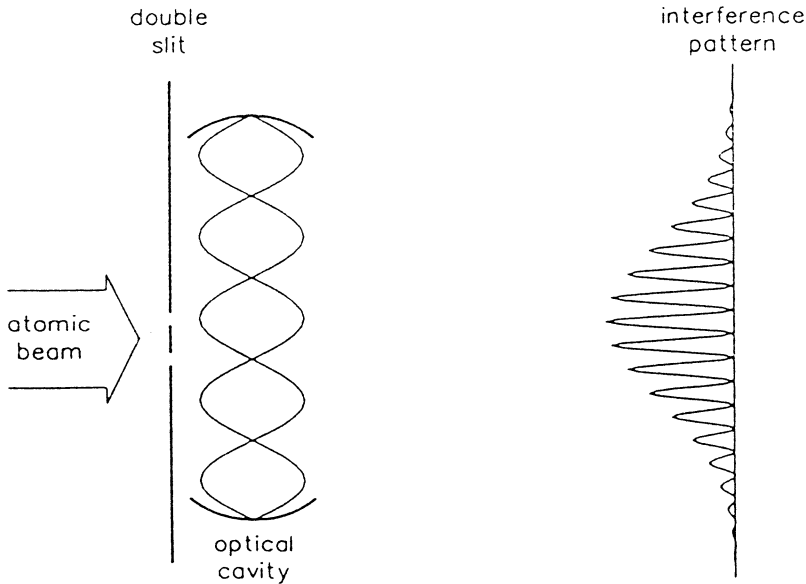

Fig. 8. Configuration for a *Welcher Weg* experiment.

a phase shift of π is induced in the field (see Fig. 10a). For a sufficiently high field intensity, a measurement of the amplitude quadrature X reveals the phase of the field, and determines which slit the atom passes through. The field measurement collapses the wavefunction of the atom so that its position distribution is localised about that slit. Consequently the atom diffracts, but no interference is observed in the far field.
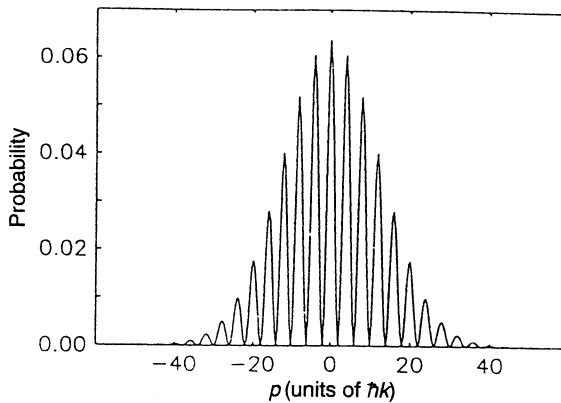
Fig. 9. Atomic momentum distribution for a double-slit interference experiment in the absence of a cavity. The slits are separated by a distance $\lambda/4$.

Suppose now that the cavity is present but that no measurement is made on the field after the interaction, so that no path information is obtained. Mathematically this situation is modelled by tracing over the field. The calculation of the far-field distribution is equivalent to adding up the *probability* distributions resulting from all possible field measurements. Because the measurement of any probable value for the amplitude quadrature localises the atom at one of the two slits, resulting in loss of interference, the sum of the far-field distributions resulting from all such measurements exhibits no interference (see Fig. 10*b*).

In the case where the cavity is present but no field measurement is made, we may think of the loss of interference as being due to the *availability* of path information. During the interaction with the standing wave, path information has been encoded in the field, and is available by means of a field measurement. Whether or not we choose to extract the information has no bearing on the physical situation and the interference fringes disappear.

Now suppose that the field amplitude is reduced. As was noted in Section 4, the resolving power of the scheme increases in proportion to the amplitude of the field. If the field intensity is too low, then a measurement of the amplitude quadrature cannot distinguish unambiguously which slit the atom passed through (see Fig. 11*a*). Due to the incompleteness of the path information recorded in the field, partial interference is restored (see Fig. 11*b*).

Instead of thinking of the loss of interference in the presence of the cavity as being due to the availability of *Welcher Weg* information, we may attribute it to random momentum kicks suffered by the atom as it scatters from photons in the cavity. A momentum kick will deflect the atom and shift the whole interference pattern across the screen. Random momentum kicks can thereby smear out the interference pattern. The magnitude of the momentum kicks needed to wash out the interference pattern is $2\hbar k$, which is exactly the momentum transferred between the atom and the field during one virtual atomic transition. As the field intensity is reduced, the atom has a lower probability of scattering from a photon in the field, and hence the interference fringes return.
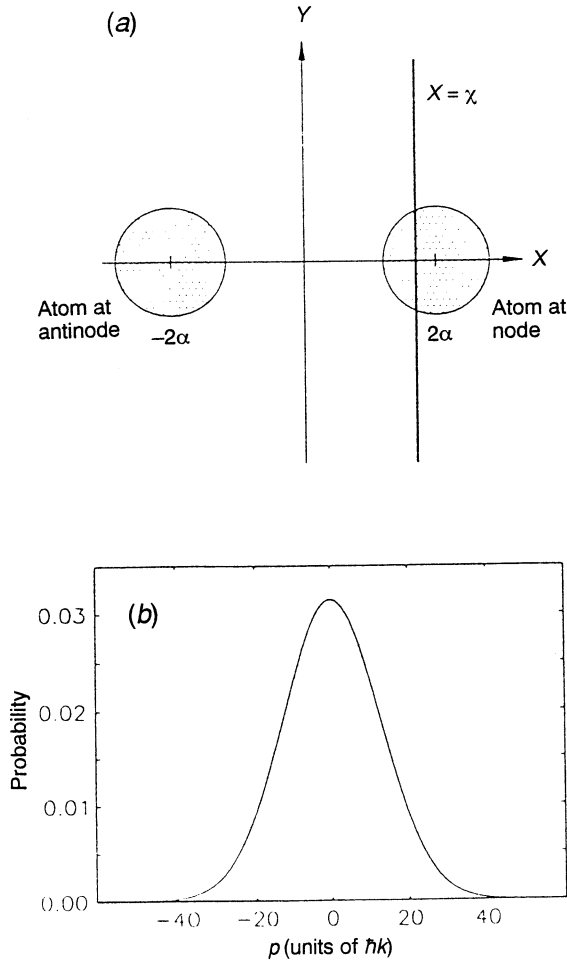
Fig. 10. (a) An atom passing through a node of the standing wave does not affect the field. An atom passing through an antinode changes the phase of the field by π. The path information can be extracted by measuring the amplitude quadrature X of the field. (b) The momentum distribution of the atom after it has passed through a standing wave of initial amplitude $\alpha = \sqrt{8}$ and no field measurement has been made.

The Quantum Eraser

It has been shown that path information about the atom is recorded in the field by the interaction in the cavity. If instead of measuring the amplitude quadrature X of the field after the interaction we choose to measure the phase quadrature Y, no path information is revealed (see Fig. 12a). In fact, the path information is erased permanently, as by a quantum eraser (Scully and Drühl 1982).

Fig. 12b shows the far-field distribution resulting from two possible measurements of the phase quadrature Y. In each case the *Welcher Weg* information is erased, and complete interference is seen in the far field. The position of the fringes depends on the particular value measured for Y, and if the far-field distributions resulting
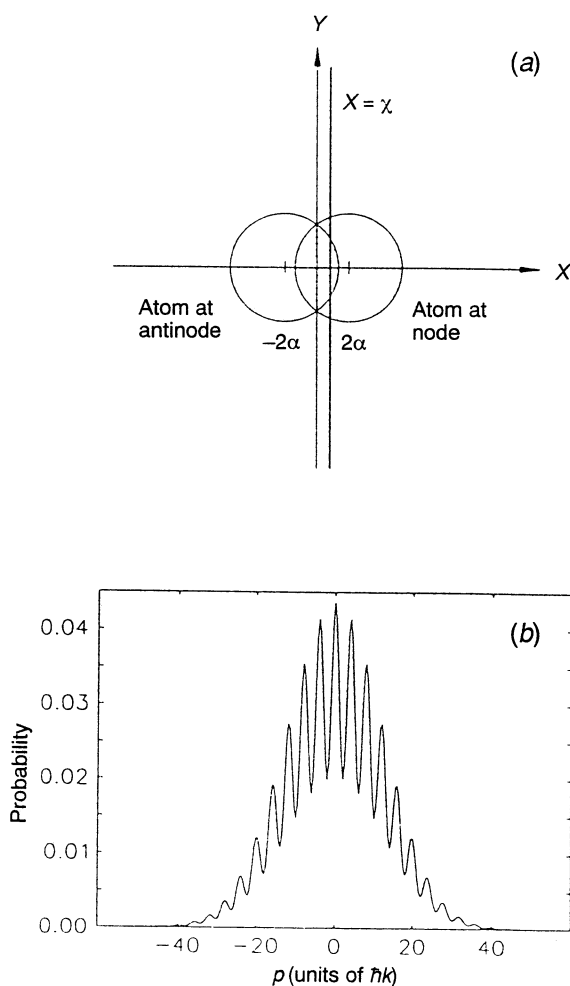
Fig. 11. (*a*) For a low field intensity, the measurement of
the amplitude quadrature cannot determine unambiguously
whether the atom passed through a node or an antinode of
the standing wave. (*b*) Atomic momentum distribution after
passing through a standing wave ($\alpha = \sqrt{0 \cdot 5}$) and no field
measurement has been made.

from all the possible measurements are summed, the resulting 'no-measurement'
distribution exhibits no interference fringes.

For a sufficiently high field intensity, a measurement of the amplitude quadrature
X can be considered to reveal the particle-like behaviour of the atom, because
it specifies a unique slit through which the atom passed. On the other hand, a
measurement of the phase quadrature Y can be considered to reveal the wave-like
behaviour of the atom, since the conditional far-field distribution for a particular
Y measurement exhibits interference. The experimentalist may delay the decision
whether to display wave-like or particle-like behaviour until after the atom–field
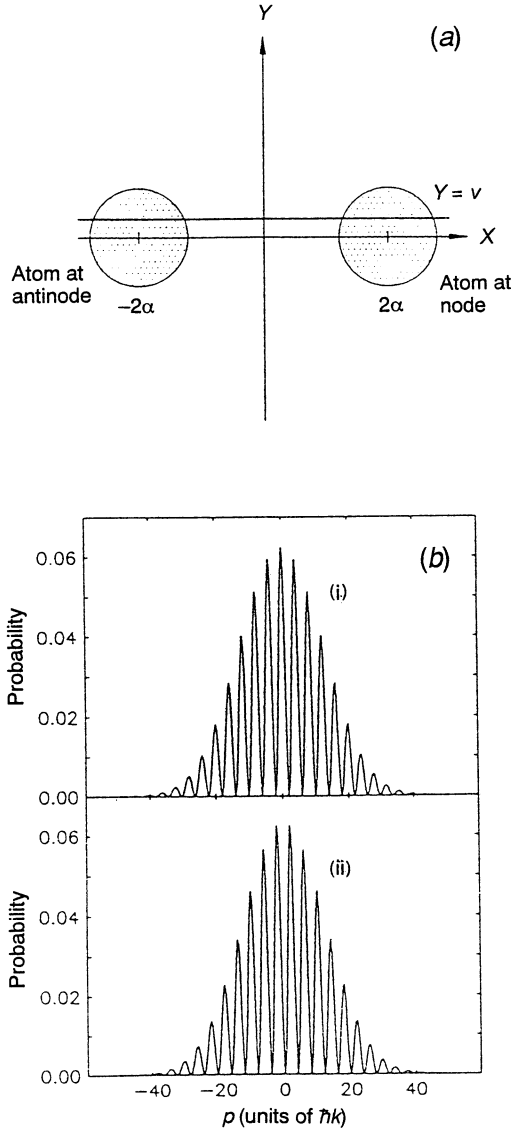interaction, when the atom can no longer be physically manipulated.

Fig. 12. Quantum eraser: (a) No path information is revealed by a measurement of the phase quadrature Y. (b) The interference pattern resulting from (i) the measurement $Y = 0$ is in antiphase with the pattern resulting from (ii) the measurement $Y = \pi/2\alpha$ ($\alpha = \sqrt{8}$).

6. Continuous Measurement of Atomic Position

In the previous section the position of an atom passing quickly through a standing-wave light field was determined by measuring the phase imparted to the light field. The transverse motion of the atom whilst in the light field was neglected. We now consider the situation where the atom spends a longer time

in the light field so that the transverse motion cannot be neglected. By making continuous measurements on the quadrature phase of the output light from the standing wave cavity, we are able to continuously monitor the transverse motion of the atom. The continuous measurement is modelled using Monte Carlo simulation techniques described by Wiseman and Milburn (1993) and by Carmichael (1993).

We consider a two-level atom interacting with a quantised cavity field mode. In the large detuning limit the effective interaction Hamiltonian is given by (15). The cavity decay rate is γ_{cav} and the cavity is driven with a coherent driving field of amplitude β. A homodyne measurement is performed on the phase quadrature $X_{\pi/2} = i(a - a^\dagger)$ of the output field from the cavity. Due to the assumption of a large detuning, spontaneous emission is neglected. A calculation including spontaneous emission is given by Quadt *et al.* (1995).

Using the method of quantum trajectories the evolution of this system is described by the unnormalised stochastic Schrödinger equation:

$$\mathrm{d}\left|\psi_c\right\rangle = \left\{\left[\frac{-i}{\hbar} H_{\mathrm{eff}} - i\sqrt{\gamma_{\mathrm{cav}}}\left(\sqrt{\gamma_{\mathrm{cav}}}\left\langle X_{\pi/2}\right\rangle + \xi\right) a\right]\mathrm{d}t\right\}\left|\psi_c\right\rangle, \qquad (60)$$

where

$$H_{\mathrm{eff}} = \frac{p^2}{2m} + \hbar\Delta\sigma_{\mathrm{z}} - \frac{i\hbar\gamma_{\mathrm{cav}}a^\dagger a}{2} + i\hbar\sqrt{\gamma_{\mathrm{cav}}}\,\beta(a^\dagger - a) \qquad (61)$$

is a non-Hermitian effective Hamiltonian, ξ represents Gaussian white noise, and the term $\sqrt{\gamma_{\mathrm{cav}}}\left(\sqrt{\gamma_{\mathrm{cav}}}\left\langle X_{\pi/2}\right\rangle + \xi\right)$ is proportional to the measured photocurrent and is conditioning the system on the measurement. In order to compensate for cavity losses and maintain a stable intracavity intensity, the cavity is driven by a coherent driving field with amplitude β:

$$\beta = \tfrac{1}{2}\sqrt{\gamma_{\mathrm{cav}}}\,\alpha\,, \qquad (62)$$

where α is the amplitude of the original coherent state in the cavity.

The stochastic Schrödinger equation (60) describes the time evolution of the quantum trajectory wavefunction $\left|\psi_{\mathrm{c}}\right\rangle$. The subscript c indicates the fact that we are dealing with a conditioned wave function. It describes the state of the open system (atom plus cavity field) at time t, conditioned on the particular history of measurement records recorded at the detectors monitoring the system prior to t. The conditioning of the system due to the homodyne detection of the output field of the cavity is modelled by a quantum diffusion process. In homodyne detection the output field is added coherently at a beamsplitter to a strong local oscillator field. This field is detected by a photoelectron detector. The measurement record is a stochastic photocurrent,

$$I(t) \propto \sqrt{\gamma_{\mathrm{cav}}}\left[\sqrt{\gamma_{\mathrm{cav}}}\left\langle X_{\pi/2}(t)\right\rangle + \xi(t)\right]\,. \qquad (63)$$

The connection between a single quantum trajectory $\left|\psi_{\mathrm{c}}(t)\right\rangle$ and the solution of the corresponding master equation $\rho(t)$ is given by $\rho(t) = \left\langle\left|\tilde{\psi}_{\mathrm{c}}(t)\right\rangle\left\langle\tilde{\psi}_{\mathrm{c}}(t)\right|\right\rangle$, where
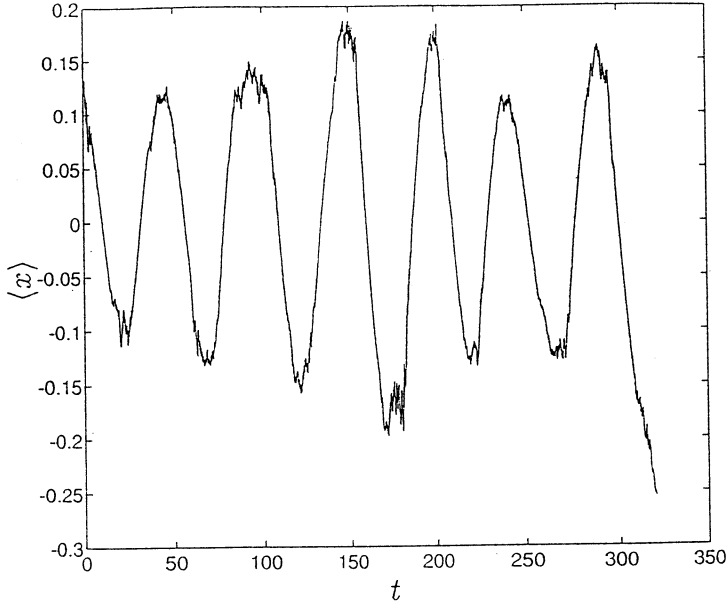
Fig. 13. Centre-of-mass motion of an atom in a cavity light field.
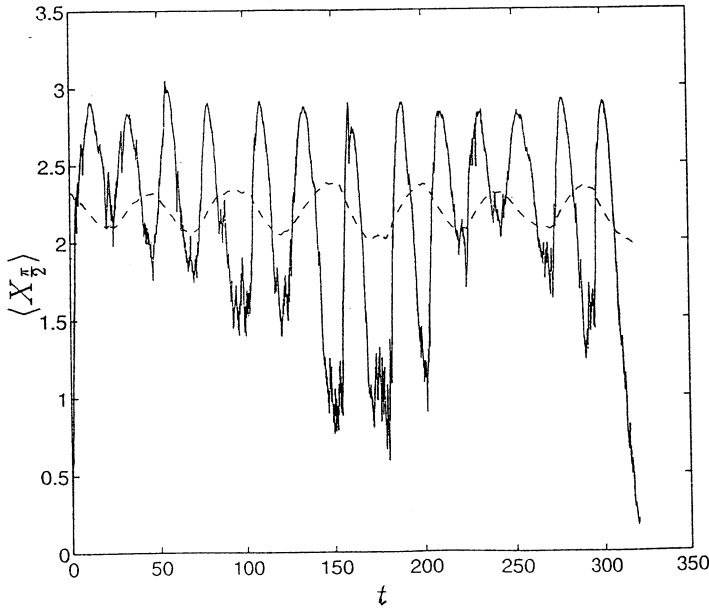

Fig. 14. Relation between the phase quadrature $\left\langle X_{(\pi/2)}(t) \right\rangle$ of the light (solid curve) and the centre-of-mass motion of the atom $\left\langle x(t) \right\rangle$ (dashed curve).

$\langle \cdots \rangle$ denotes the ensemble average over realisations of the two stochastic processes. Our objective is to show the relation between the measured photocurrent and the transverse motion of an atom in the cavity field. This implies that we are more interested in the properties of a single quantum trajectory than in the solution of the master equation because $\rho(t)$ does not describe a particular measurement scheme, that is, different measurements (for example, the measurement of the amplitude instead of the phase quadrature) result in the same master equation.

We have simulated the motion of a caesium atom using the quantum trajectory technique. The active atomic transition is chosen to be the $6S_{1/2}$, $F = 4 \rightarrow 6P_{3/2}$, $F = 5$ transition which has a wavelength $\lambda = 852$ nm. We choose the experimental parameters of Kimble (1994) for the atom–field coupling constant $g = 7 \cdot 16$ MHz and the cavity lifetime $\tau_{\text{cav}} = 0 \cdot 18\,\mu$s. This high field coupling and long cavity lifetime are necessary for effective monitoring of the atomic motion. We choose for the detuning $\Delta = 26\gamma_{\text{A}}$, where $\gamma_{\text{A}} = 32 \cdot 3 \times 10^6$ rad s^{-1}. The choice of detuning is a compromise between a reasonably large effective interaction strength g^2/Δ and suppressing the spontaneous emission. The amplitude of the initial cavity field state is chosen to be $\alpha = 3$.

Fig. 13 shows the centre-of-mass motion of an atom in the cavity light field. The expectation value $\langle x \rangle$ in units of wavelength of the cavity field is plotted against time in units of cavity decay times. The total time of the simulation is $320/\gamma_{\text{cav}}$. The atom initially starts halfway between a node and antinode of the standing light field, where '0' in the figure indicates the location of an antinode. The initial state is a Gaussian wavefunction with standard deviation $\sigma = \lambda/20$, i.e. the atom starts well localised in the potential well. The figure shows an oscillatory motion of the atom in the potential $-(g^2/\Delta)\,a^\dagger a \cos^2 kx$. This oscillation would be washed out by averaging over many trajectories since each would start with a different value of $\langle x \rangle$.

Fig. 14 shows the relation between the expectation value of the phase quadrature $\langle X_{\pi/2} \rangle$ (solid curve) and the centre-of-mass motion of the atom $\langle x \rangle$ (dashed curve). The measured photocurrent is given by $\langle X_{\pi/2} \rangle$ plus white noise. It can be seen in Fig. 14 that the phase quadrature is oscillating with double the frequency of the centre-of-mass motion. Here $\langle X_{\pi/2} \rangle$ is greatest if the atom is located in the minimum of the potential and least if the atomic position is closest to a node of the standing wave, i.e. at the turning points of the motion. The amplitude of the oscillations of $\langle X_{\pi/2} \rangle$ is related to the amplitude of $\langle x \rangle$. However, the amplitude of the atomic motion is random, that is, it differs from trajectory to trajectory.

References

Adams, C. S., Sigel, M., and Mlynek, J. (1994). *Phys. Rep.* **240**, 143.

Bohr, N. (1935). *Phys. Rev.* **48**, 696.

Braginsky, V. B. (1988). *Sov. Phys. Usp.* **31**, 836.

Brune, B., Haroche, S., Lefevre, V., Raimond, J. M., and Zagury, N. (1990). *Phys. Rev. Lett.* **65**, 976.

Carmichael, H. J. (1993). 'An Open Systems Approach to Quantum Optics', Lecture Notes in Physics (Springer: Berlin).

Caves, C. M., Thorne, K. S., Drever, R. W. P., Sandberg, V. P., and Zimmerman, M. (1980). *Rev. Mod. Phys.* **53**, 341.

Gardner, J. R., Marable, M. L., Welch, G. R., and Thomas, J. E. (1993). *Phys. Rev. Lett.* **70**, 3404.

Grangier, P. (1991). *Phys. Rep.* **219**, 121.

Herkommer, M., Akulin, V. M., and Schleich, W. P. (1992). *Phys. Rev. Lett.* **69**, 3298.

Holland, M. J., Walls, D. F., and Zoller, P. (1991). *Phys. Rev. Lett.* **67**, 1716.

Kimble, H. J. (1994). *In* 'Cavity Quantum Electrodynamics', Adv. At. Mol. Opt. Phys., Suppl. 2 (Ed. P. R. Berman) (Academic: San Diego).

Mabuchi, H., and Kimble, H. J. (1994). *Opt. Lett.* **19**, 749.

Marte, M., and Zoller, P. (1992). *Appl. Phys.* B **54**, 477.

Matsko, A. B., Vyatchanin, S. P., Mabuchi, H., and Kimble, H. J. (1994). *Phys. Lett.* A **192**, 175.

Meystre, P., Schumacher, F., and Stenholm, S. (1989). *Opt. Commun.* **73**, 443.

Quadt, R., Collett, M. J., and Walls, D. F. (1995). *Phys. Rev. Lett.* **74**, 351.

Salomon, C., Dalibard, J., Aspect, A., Metcalf, H., and Cohen-Tannoudji, C. (1987). *Phys. Rev. Lett.* **59**, 1659.

Scully, M. O., and Drühl, K. (1982). *Phys. Rev.* A **25**, 2208.

Sleator, T., Pfau, T., Balykin, V., and Mlynek, J. (1992). *Appl. Phys.* B **54**, 375.

Storey, P., Collett, M., and Walls, D. F. (1992). *Phys. Rev. Lett.* **68**, 472; *Phys. Rev.* A **47**, 405 (1993).

Storey, P., Sleator, T., Collett, M., and Walls, D. F. (1994). *Phys. Rev.* A **49**, 2322.

Treussart, F., Hare, J., Collot, L., Lefevre, V., Weiss, D., Sandogher, V., Raimond, J. M., and Haroche, S. (1994). *Opt. Lett.* **19**, 1651.

Wallis, H. (1995). *Phys. Rep.* **255**, 203.

Walls, D. F., and Milburn, G. J. (1994). 'Quantum Optics' (Springer: Berlin).

Wilkens, M. (1996). 'De Broglie Optics', Atomic, Molecular and Optical Physics Reference Book (AIP, to be published).

Wiseman, H. M., and Milburn, G. J. (1993). *Phys. Rev.* A **47**, 642.

Yuen, H. P. (1983). *Phys. Rev. Lett.* **51**, 719.